The Anti-Static Poly(ethylene terephthalate) Nanocomposite Fiber by *In Situ* Polymerization: The Thermo-Mechanical and Electrical Properties

Xiaolei Chen,[1] Chunzhong Li, Wei Shao,[1] H. L. Du,[2] J. S. Burnell-Gray[2]

[1]*Key Laboratory for Ultrafine Materials of Ministry of Education, School of Materials Science and Engineering, East China University of Science and Technology, Shanghai 200237, People's Republic of China*
[2]*Advanced Materials Research Institute, Northumbria University, Newcastle upon Tyne NE1 8ST, United Kingdom*

Received 6 July 2006; accepted 8 January 2007
DOI 10.1002/app.26381
Published online 23 April 2007 in Wiley InterScience (www.interscience.wiley.com).

ABSTRACT: Poly(ethylene phthalate) (PET)/nano-antimony doped tin oxide (ATO) composites prepared via *in situ* polymerization were spun into fiber by the melt-spinning process. ATO were in the form of loose agglomeration dispersing in the PET fibers and the sizes of loose agglomeration were smaller than 150 nm. Comparing with the neat PET, the tenacity of PET/ATO hybrid fibers was improved, and PET/ATO hybrid fibers had a lower elongation at break by adding nano-ATO. The percolation threshold of PET/ATO hybrid fibers at room temperature was as low as 1.05 wt %, much lower than that of the composites filled with conventional conductive particles. The PET/ATO hybrid fiber exhibited volume resistivity of 4.9×10^8 Ω cm when the contents of ATO were 1 wt %. The ATO nanoparticles improved the thermal stability of PET fiber. The WAXD and DSC results suggested that ATO nanoparticles increase the degree of crystallinity of PET acting as the nucleating agent, which prohibited the thermal shrinkage of PET fiber. © 2007 Wiley Periodicals, Inc. J Appl Polym Sci 105: 1490–1495, 2007

Key words: antistatic; fibers; nanocomposites; poly(ethylene terephthalate); thermal stability; antimony doped tin oxide

INTRODUCTION

Organic/inorganic hybrids have generated substantial recent interest as a result of their potential as single molecular-scale composites with desirable organic and inorganic characteristics and new properties arising from the interaction between the two components.[1–4] Poly(ethylene terephthalate) (PET) is a material with low cost and high performance, which has been found wide applications in fiber and nonfiber fields. However, the high specific resistance (more than 10^{14} Ω cm) and the static problem of PET will restrict its further application of PET. At present, the antistatic PET fibers were prepared mostly by adding conducting nanoparticles and the incorporation can result in materials possessing permanent antistatic property.[5,6]

Antimony doped tin oxide (ATO) exhibits both optical transparency to visible radiation and high electrical conductivity. ATO has been intensively studied for its high-temperature, chemical and mechanical stabilities.[7] At low Sb doping level, the conductivity of ATO is greatly increased as compared to pure tin oxide and can be varied easily by changing the Sb doping level.[8] When used as antistatic agent, ATO shows better performance than the currently used carbon blacks, metallic pigment and organic polymer binders.[9] A novel fabric finishing agent containing ATO has been prepared and used for antistatic treatment for PET fabric.[10] The surface resistance of PET fabric treated by the novel finishing agent could be decreased from 10^{12} to 10^{10} Ω.

In the preparation of nanocomposites, the key issue is the dispersion of nanoparticles or eliminating the aggregation of nanoparticles. Many efforts have been made to solve this problem. The available methods include the sol–gel blending technique,[11] the melt-blending process,[12] the *in situ* polymerization process,[13–15] and the *in situ* forming nanoparticles process.[16] Among these methods, the *in situ* forming nanoparticle process is the most reasonable and effective because it can produce single particle dispersion composites. However, the *in situ* forming nanoparticle process can only be used for those systems in which no transformation of the crystal morphology of nanoparticles is needed at high temperature because the matrix polymer usually cannot endure high temperature.

Thus, to improve the dispersion of ATO nanoparticles in the PET matrix, we developed an *in situ* polymerization process to produce the PET/ATO nanocomposites. In this process the ATO nanoparticles were

Correspondence to: C. Li (czli@ecust.edu.cn).

TABLE I
Characteristics of the ATO Sample

Sample	ATO
BET surface area (m^2/g)	65
Average particle size (nm)	20
Volume resistivity (Ω cm)	1–5

first treated with a coupling agent to introduce some organic functional groups onto the surface of the ATO nanoparticles; then the nanoparticles were dispersed in ethylene glycol (EG); and, finally, EG reacted with terephthalic acid (PTA), thus going to polycondensation in the presence of ATO nanoparticles to form PET/ATO nanocomposites.

Up to now, only a few studies have been reported on the spinning of polymer/ATO nanocomposites. In this article, the PET/ATO nanocomposite was prepared through *in situ* polymerization, and then the acquired material was produced to fibers by melt spinning. The structure and properties of this material and its fibers were studied in detail.

EXPERIMENTAL

Materials

ATO nanoparticles were prepared by the chemical coprecipitation method which had been described previously,[17] and its characteristics were listed in Table I. Ethylene glycol (EG), cobalt acetate (as catalyst), antimony trioxide (as catalyst), terephthalic acid (PTA) were kindly supplied by Shanghai Chemical Fiber Institute.

Synthesis of PET/ATO nanocomposites

The PET/ATO nanocomposites were synthesized with 2 L reactor. ATO nanoparticles were modified by silane coupling agent and dispersed in EG by ball-milling at 25°C. Since the synthetic procedures for all of the hybrids were almost the same, only a representative example, the procedure for the preparation of nanocomposites containing 1 wt % ATO, is given here. In the 2 L reactor, 403 g of EG (with 12.7 g of modified ATO), 830 g of PTA, 0.017 g of cobalt acetate, and 0.248 g of antimony trioxide were placed. This mixture was first agitated at 30 rpm at room temperature. This mixture was then heated in nitrogen atmosphere from room temperature to 250–260°C under a pressure of 1.5×10^5 Pa to esterify it. During the esterification, the pressure was slowly reduced to air pressure to emit the water generated. Afterward, the polymerization was carried on at 270–280°C, and the pressure of polymerization was gradually reduced up to 70 Pa. A power meter was used to denote the polymerization level. When the power meter increases to 50%, for each sample, time has little difference; with changes from 120 to 150 min, the agitation was stopped. Finally, the melting polymer was extruded through an orifice at the N_2 pressure of 1.5 kg and cooled with water. The neat PET and PET with different ATO contents were fabricated by the same process.

Spinning

The materials were dried *in vacuo* for 48 h at 120°C prior to spinning. The neat PET and PET/ATO nanocomposites were spun into fiber with 36 monofilaments on an ABE-25 spinning machine at the take-up speed of 1200 m/min; the temperatures in the screw region are listed in Table II. Then the drawing of fiber was carried out on a Barmag3013 drawing device at a temperature of 160°C with a draw ratio of 3.8.

Characterization

Scanning electron microscope

The morphologies of the surface of PET/ATO fiber samples were investigated using Model JSM-6360LV scanning electron microscope (SEM). An SPI sputter coater was used to sputter-coat the surfaces with gold for enhanced conductivity.

Transmission electron microscope

All fiber samples were first put into epoxy capsules and then the curing of the epoxy at 70°C for 24 h *in vacuo*. The cured epoxies containing the PET hybrids were sectioned into 80–100 nm thin slices by an ultramicrotome. The dispersion of ATO in PET fiber was observed by Model H-600 (Hitachi, Tokyo) transmission electron microscope (TEM) using an acceleration voltage of 120 kV.

Tensile test

The mechanical properties of PET/ATO fibers were measured using an AGS materials testing machine with a gauge length of 250 mm at 25°C. An average of at least 10 individual determinations was obtained.

Electrical property measurements

The electrical properties of the fibers were measured with a specific resistance tester (Model YG321) at

TABLE II
Spinning Technical Parameters of PET/ATO Nanocomposites

Section no.	Screw				Spinning pump	Spinning beam
	1	2	3	4		
Temperature (°C)	287	305	300	300	300	310

25°C. An average of at least 10 individual determinations was obtained.

Thermal shrinkage test

One end of each fiber sample was fixed, and another end was loaded certain stress that related to fiber's denier, the original length, L (mm), of fiber being marked. All fiber samples were kept at various environmental temperatures for 30 min, and then the length, L_1 (mm), between the two marks of each fiber sample was measured. The thermal shrinkage was calculated according to the following equation:

$$\text{Thermal shrinkage (\%)} = \frac{L-L_1}{L} \times 100$$

Differential scanning calorimeter

The thermal behavior was studied by differential scanning calorimeter (DSC) (Model Netzsch PC200). The temperature of the instrument was calibrated with indium, and the baseline was checked by using sapphire. All tests were performed in nitrogen atmosphere. All samples were heated first to 300°C at 10°C/min to study the melting of the neat PET and PET/ATO fibers and kept for 10 min in the hermetic cell. The samples were then auto cooled at 10°C/min to 100°C to study the crystallization of the neat PET and PET/ATO fibers.

X-ray diffraction

X-ray diffraction (XRD) was analyzed by X-ray diffraction (XRD) (Model D/MAX-2550PC) in the reflection mode at 40 kV and 40 mA with a Cu target and Ni filter. The 2θ angle range was between 5° and 40°.

The crystallinity measurement by XRD is based on the Vainshtein intensity conservation law. The total intensity of diffraction is the summation of intensity both in crystalline region and in amorphous region; thus the crystallinity of fiber is calculated as follows[18]:

$$X_c = \frac{\int_0^\infty S^2 I_c(s) ds}{\int_0^\infty S^2 I(s) ds} \quad (1)$$

where X_c is the crystallinity of fiber; $S = 2\sin\theta/\lambda$; $I(s)$ is the total intensity of diffraction; $I_c(s)$ is the intensity of diffraction in crystalline region.

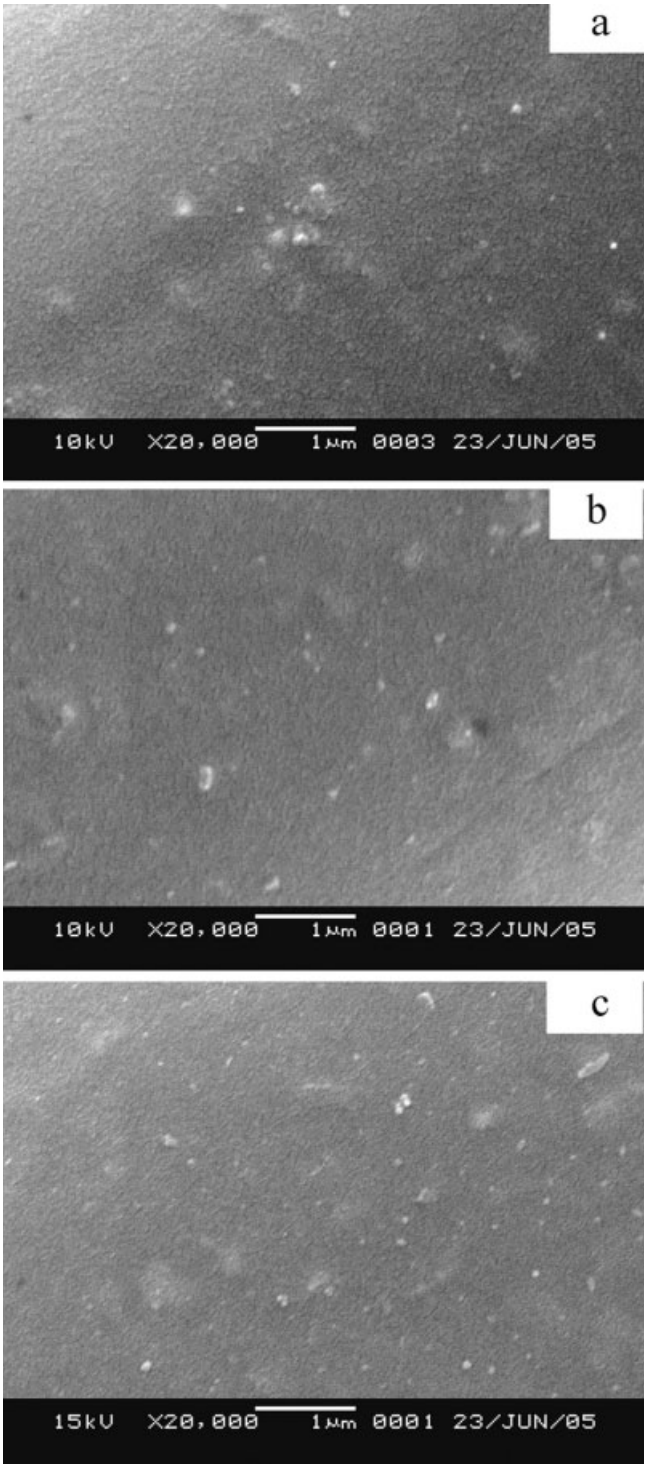

Figure 1 SEM micrographs of PET/ATO hybrid fibers: (a) PET with 0.5 wt % ATO; (b) PET with 1 wt % ATO; (c) PET with 1.8 wt % ATO.

RESULTS AND DISCUSSION

Morphology of PET/ATO hybrid fibers

Figure 1 showed the SEM images of the PET/ATO hybrid fibers surface with different ATO contents. As these images showed, the ATO particles were well dispersed in the fibers surface. Although some ATO particles aggregated in the matrix, the average agglomeration diameter typically was below 150 nm. Inorganic nanoparticles are hard to disperse in polymer matrix because of particle agglomeration and immiscibility between the inorganic particles and the polymer matrix. So, the ATO was first modified by silane coupling agent and well dispersed in the solution

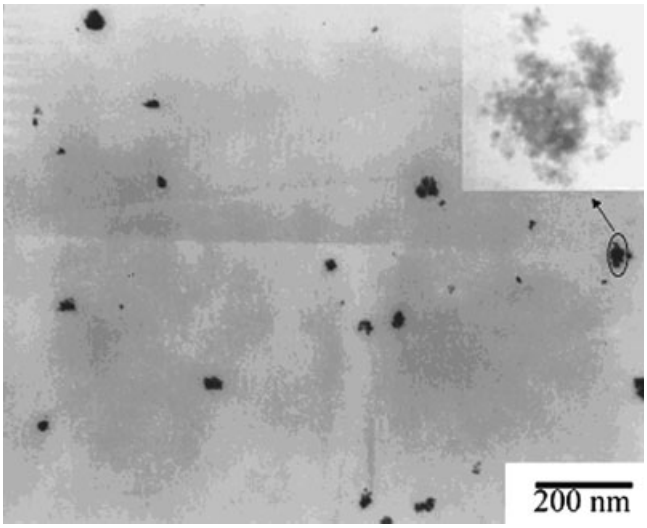

Figure 2 TEM micrograph of PET hybrid fibers with 1 wt % ATO.

of EG by ball-milling. PET/ATO nanocomposites were prepared by means of esterification and polycondensation reactions of TPA and EG of ATO nanoparticles. Modification method of ATO by silane coupling agent and using EG as a media of mixture in a ball-milling mixing could provide better dispersion of ATO in PET.

More direct evidence of the formation of true fibers is provided by the TEM images of an ultramicrotomed section. Figure 2 showed photographs of PET hybrid fibers containing 1 wt % ATO. A TEM allows a qualitative understanding of the internal structure through direct observation. Figure 2 showed that ATO particles were bonded tightly to PET matrix and well dispersed in the PET continuous phase in the form of loose agglomeration, which had many branched chains and more easily form conducting network structure. And the sizes of the agglomeration were smaller than 150 nm.

Electrical property of PET/ATO hybrid fibers

Variations of the electrical conductivities of neat PET and the PET/ATO hybrid fibers with respect to ATO content were shown in Figure 3. The resistances (R) of the hybrid fibers were measured by specific resistance tester and the specific resistance (ρ_v) of the hybrid fibers were obtained from R, using the relation:

$$\rho_v = 12R\,f$$

where f is the standard compactedness of the fiber. f is 0.23 for the PET fiber.

Figure 3 showed that when ATO was increased from 0 to 8 wt % in hybrid fibers, the electrical properties of the fibers improved from 2.7×10^{13} to 3.7×10^{8}

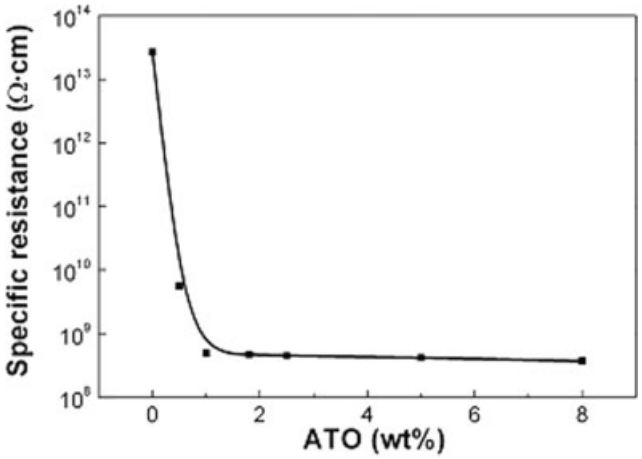

Figure 3 Effect of ATO contents on the specific resistance of the hybrid fibers.

Ω cm. For PET/ATO hybrid fibers, an abrupt conductivity transition occurred at a critical ATO content, which can be designated as the percolation threshold. The fibers containing ATO nanoparticles exhibited a percolation threshold about 1.05 wt %; whereas the composites filled by other conductive powder possessed a much higher threshold concentration.[19] The advantage of ATO over conventional conductive powder was significant. This was consistent with the observation in Figures 1 and 2: ATO was not in form of single particle dispersing in PET matrix, but in the form of loose aggregates. These aggregates were chain structure composed of several ATO particles, which were elementary unit of ATO in PET matrix. More short chains existed in the loose aggregates and were more easily prone to form conductive network.[20]

Mechanical property of PET/ATO hybrid fibers

Because the PET/ATO hybrid fiber containing 1 wt % ATO is up to the demand of antistatic fiber, the mechanical properties only compare the PET/ATO hybrid fiber containing 1 wt % ATO to the neat PET fiber. The mechanical properties of PET and PET/ATO hybrid fiber are listed in Table III. According to the data shown in Table III, incorporation of ATO has some advantageous effects on fibers; the tenacity and

TABLE III
Properties of Neat PET and PET/ATO Fibers

Sample	Neat PET fibers	PET hybrid fibers
Stretch ratio	3.8	3.8
Linear density (dtex)	123.0	121.2
Tenacity (cN/dtex)	3.01 ± 0.13	3.29 ± 0.14
Tensile strength at 5% elongation (cN/dtex)	2.00 ± 0.11	2.24 ± 0.10
Strain at Max (%)	29.9 ± 1.5	25.3 ± 1.3

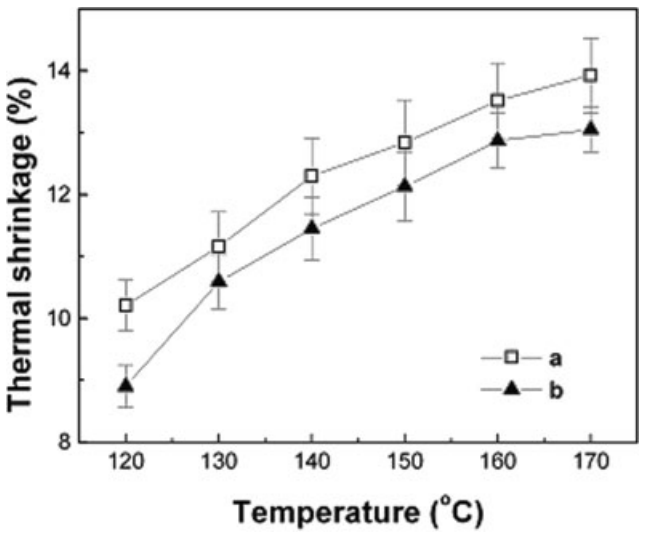

Figure 4 Thermal shrinkage of fibers at various environmental temperatures: (a) neat PET; (b) PET with 1 wt % ATO.

the tensile strength at 5% elongation of PET/ATO hybrid fibers were improved. The reason may be that the ATO nanoparticles dispersed uniformly in PET matrix slightly restricted the movement of PET macromolecules.[21] At the same time, the elongation at break of fiber slightly decreased with the addition of ATO. It was assumed that the addition of ATO nanoparticles resulted in decreased interaction between the PET macromolecules.

Thermal shrinkage of PET/ATO hybrid fibers

Figure 4 showed that the thermal shrinkage of fiber increased as the environment temperature increased. This was because the disorientation of PET molecular chains occurred more easily while the environmental temperature was increased. It was also observed that the thermal shrinkage of PET/ATO fiber was lower

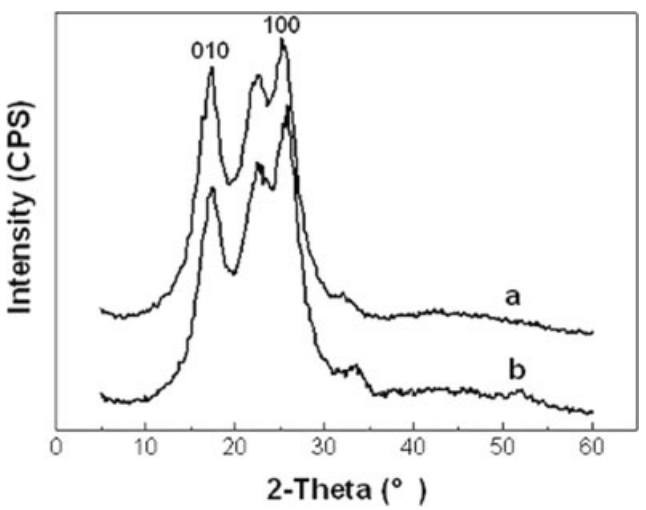

Figure 5 XRD patterns of fibers heated at 150°C for 30 min: (a) neat PET; (b) PET with 1 wt % ATO.

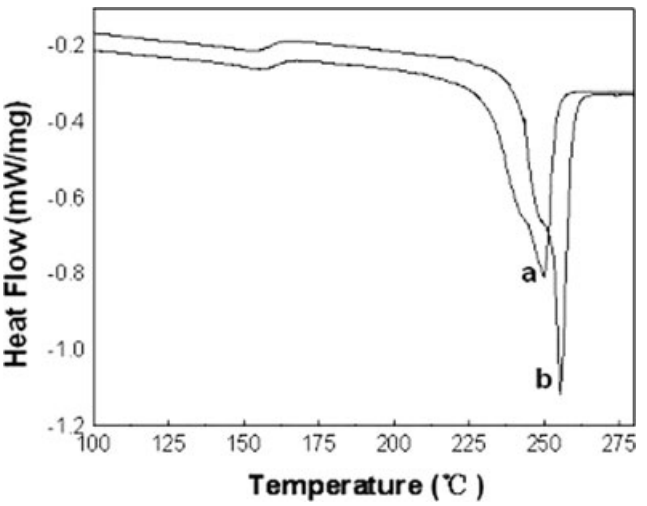

Figure 6 Heating measurement of DSC trace for fibers heated at 150°C for 30 min: (a) neat PET fibers; (b) PET with 1 wt % ATO.

than that of neat PET fiber. As we know, during the drawing of fiber, the molecular orientation increases in the amorphous phase and the molecular chains transform from random entangled state to extension, which results in the decrease of entropy. Therefore the system is unstable in thermodynamics and has an internal drive to disorient. High crystallinity and proper crystal size as well as good crystal distribution of fiber can lead to higher dimension stability.[22]

Thermal property of PET/ATO hybrid fibers

We performed XRD experiments on neat PET and the PET/ATO hybrid fibers, which are both heated at 150°C for 30 min. The results are shown in Figure 5.

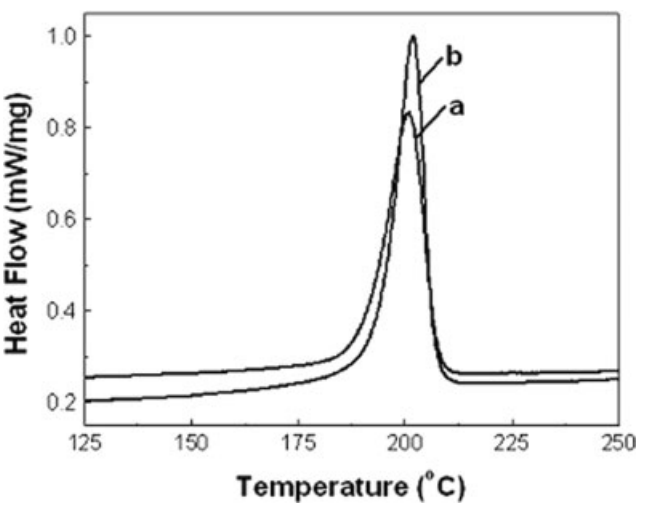

Figure 7 Cooling measurement of DSC trace for fibers heated at 150°C for 30 min: (a) neat PET fibers; (b) PET with 1 wt % ATO.

TABLE IV
DSC Data for Neat PET and PET/ATO Fibers

	Heating			Cooling		
Sample	T_{onset} (°C)	T_m (°C)	ΔH_f (J/g)	T_{onset} (°C)	ΔT_c (°C)	ΔH_c (J/g)
Ncat PET fiber	229.5	249.9	41.90	190.8	200.9	38.77
PET/ ATO fiber	252.0	255.4	43.31	193.9	202.0	42.69

The neat PET and hybrid PET both showed obvious diffraction peak. The crystallinity of neat PET fiber and PET/ATO hybrid fiber were 48.5 and 53.8%, respectively, which were calculated according to eq. (1). It could be seen that crystallinity of PET increased with adding ATO.

To further investigate the influence of nanoparticles ATO on the crystallization of PET, neat PET, and PET/ATO hybrid fibers were measured by DSC. Before measuring by DSC, the samples are both heated at 150°C for 30 min. Figures 6 and 7 showed the heating and cooling curves of neat PET and PET/ATO hybrid fibers, respectively. The symbols and resulting data of samples are listed in Table IV. Comparing the neat PET fibers, the T_m values of hybrid fibers are higher, which implied that the crystal of PET/ATO fibers were more stable than that of neat PET fiber. The value of ΔH_f for PET/ATO fibers is larger than that of neat PET. This reveals that the amount (degree) of crystallinity of PET increases with adding ATO.

From the results of the cooling process (see Table IV), the values of the crystallization temperature T_c values and ΔH_c for PET/ATO hybrid fibers were higher than those of neat PET. It can be explained that ATO exhibits a strong heterophase nucleation effect on PET crystallization due to its enormous surface area. These results also indicate that ATO may be an ideal nucleating agent for PET processing. The enhancement of crystallinity will result in the decrease of the disorientation of molecular chains in the amorphous region, which represents the macroscopic improvement of dimensional stability of fiber.

Because the ATO nanoparticles are very small and they exhibit globular surface texture as shown in the TEM photomicrographs, these may also prevent intimate contact between the particles and polymer chains surrounding them, and the ATO nanoparticles cannot effectively restricted the motion of the PET molecular segment. These also could be proved that adding ATO had no apparent influence on the tenacity of PET. According to the existing research,[23] ATO nanoparticles increase the degree of crystallinity of PET acting as the nucleating agent, which chiefly led to the improvement of the heat resistance and dimensional stability of fiber. Therefore, it can be acknowledged that the thermal stability of PET fiber was improved by ATO nanoparticles.

CONCLUSIONS

PET/ATO nanocomposites prepared by *in situ* polymerization exhibited good antistatic property. In this study, the uniform dispersion of ATO in the PET fibers by this method was confirmed by SEM and TEM measurements. The electrically conductivity of PET/ATO fibers reached 4.9×10^8 Ω cm at ATO content of 1 wt %. The tensile strength of PET fibers with 1 wt % ATO content increased slightly in contrast to that of neat PET fiber; at the same time it had a lower elongation at break. The thermal dimensional stability of PET fiber was improved as a result of the addition of ATO nanoparticles. The results of microstructure investigations suggested that ATO nanoparticles increased the degree of crystallinity of PET acting as the nucleating agent, which prohibited the thermal shrinkage of PET fiber.

References

1. Giannelis, E. P. Adv Mater 1996, 8, 29.
2. Messersmith, P. B.; Giannelis, E. P. Chem Mater 1993, 5, 1064.
3. Pinnavaia, T. J. Science 1983, 220, 365.
4. Gilman, J. W. Appl Clay Sci 1999, 15, 31.
5. Gao, G. Y.; An, S. L.; Yu, J. L. J Tianjin Polytech Univ 2005, 24, 12.
6. Huang, Y.; Li, Z. F.; Luo, G. H. China Syn Fiber Ind 2004, 27, 1.
7. Rajpure, K. Y.; Kusumade, M. N.; Suallart M. N. N. N. Mater Chem Phys 2000, 64, 184.
8. Kim, K. H.; Lee, S. W.; Shin, D. W.; Park, C. G. J Am Ceram Soc 1994, 77, 915.
9. Orel, Z. C.; Orel, B.; Hodoscek, M.; Kaucic, V. J Mater Sci 1992, 27, 313.
10. Wu, Y.; Chi Y. B.; Ni, J. X. J Funct Polym 2002, 15, 43.
11. Juangvanich, N.; Mauritz, K. A. J Appl Polym Sci 1998, 67, 1799.
12. McNally, T.; Murphy, R. W.; Lew, Y. C.; Turner, J. R.; Brennan, P. G. Polymer 2003, 44, 2761.
13. Lantelme, B.; Dumon, M.; Mai, C.; Pascault, J. P. J Non-Cryst Solids 1996, 194, 63.
14. Li, Y.; Yu, J.; Guo, Z. Polym Int 2003, 52, 981.
15. Chang, J.; Kim, S. Polymer 2004, 45, 919.
16. Shen, L.; Du, Q.; Wang, H.; Zhong, W.; Yang, Y. Polym Int 2004, 53, 1153.
17. Qing, C. Y.; Luo, M. F.; Gu, H. C. J East China Univ Sci Technol 2001, 27, 261.
18. Ren, X.; Meng, J. Synth Technol Appl 1998, 13, 1.
19. Pinto, G.; Jimenez-Martin, A. Polym Compos 2001, 22, 65.
20. Zhang, Q. H.; Chen, D. J Polym Mater Sci Eng 2004, 20, 213.
21. Chang, J. H.; Mun, M. K.; Lee, I. C. J Appl Polym Sci 2005, 98, 2009.
22. Xiao, W. Z.; Yu, H. M.; Han, K. Q.; Yu, M. H. J Appl Polym Sci 2005, 96, 2247.
23. Chen, X. L.; Shao, W. J Chem Eng Chin Univ, to appear.